Modeling and Control of a System Described by the 2D-Burgers Equation*

Mehmet Önder Efe
Corresponding Author,
TOBB University,
Electrical and Electronics Engineering,
Sögütözü, Ankara, Turkey,
E-mail: onderefe@ieee.org,
Phone: +90-312-292-4064,
Fax: +90-312-292 4091

Fatih Kölmek and Hitay Özbay
Electrical and Electronics Engineering,
Bilkent University,
Bilkent, TR-06800, Ankara, Turkey,
{kolmek,hitay}@ug.bilkent.edu.tr

Abstract

Modeling and control of systems governed by Partial Differential Equations (PDE) is an ever-growing research field. Many PDE models and modeling techniques have been explited in the past. This paper considers the Proper Orthogonal Decomposition (POD) based model reduction and boundary control for 2D Burgers equation. The considered PDE is very similar to Navier-Stokes equations in its nonlinearity yet it does not contain turbulence. A feedback control scheme is developed to compensate the load disturbances by utilizing the linearized form of the low dimensional model. The simulation results have shown that the controller performs well.

Keywords: Reduced order modeling, infinite dimensional systems, disturbance attenuation

1 Introduction

Finding a representative dynamic model for spatially continuous systems is a major problem in heat and fluid flows. The reason that lies behind is tightly associated with control system synthesis, i.e. the design of best external excitation (boundary condition) such that the the manner in which the system behaves is the prescribed behavior. From a boundary controller design point of view, it is seen that PDE systems do not enjoy the classical tools of control theory directly, instead, the PDE system is preprocessed in such a way that the essential behavior is reproduced by a set of Ordinary Differential Equations (ODE) associated with some spatial eigenfunctions. Naturally, the obtained model is an approximation to the original system dynamics. The purpose of this paper is to show how complicated PDEs could be approximated by finite dimensional ODEs that can be used for boundary control system synthesis.

The two-dimensional (2D) Burgers equation is a good example to study the difficulties encountered in low dimensional modeling of infinite dimensional systems. The reason is that the involved dynamics is governed by two coupled nonlinear PDEs. This fact indicates that the efforts towards a suitable model are to deal with a significant amount of computational complexity. Referring to [1, 2], the 2D Burgers equation is described by

$$w_t + \epsilon(w \cdot \nabla)w = \mu\nabla^2 w \tag{1}$$

where $w(x,y,t) := (u(x,y,t) \;\; v(x,y,t))^T$, and $(x,y,t) \in [0,1]\times[0,1]\times[0,T]$ with T being some final time. The similarity of the vector PDE set in (1) with the Navier-Stokes equations makes the low dimensional modeling efforts worthwhile particularly for the boundary control applications in fluid dynamics. A striking example is the problem of reducing the skin friction of air vehicles through active flow control, (See [3]). However, the 2D Burgers equation can be seen as a turbulence free simplified version of Navier-Stokes equations and has been studied in the past for modeling traffic flows, shock waves and acoustic transmission. In [4, 5, 6], some variants of 2D Burgers equation have been considered with the goal of finding exact solutions under certain circumstances. Blender, on the other hand, postulates

*This work was supported in part by the AFRL/VA and AFOSR through the Collaborative Center of Control Science at the Ohio State University (Contract F33615-01-2-3154), and by the European Commission under contract no. MIRG-CT-2004-006666.

a method to obtain the solution of the PDE set in (1) iteratively, [7]. Güngör demonstrates that if suitable subalgebras can be defined, the PDE could be converted into an ODE, but it is a major problem to find such subalgebras particularly for boundary control purposes, [8]. Nishinari et al. focus on cellular automaton, which is extensively studied for developing models of traffic flow, fluids and immune systems, [9], and therefore a good model to work on is a variant of Burgers equation. In [10], the dynamics that arises upon discretization of 2D Burgers equation is analyzed. The effects of chosen time step (Δt) for getting physically reasonable numerical solutions are elaborated. Wescott et al. present a computational technique to obtain the numerical solutions of PDEs having nonlinear convection terms like 2D Burgers equation and Navier-Stokes equations, [11]. The goal of the paper is to reduce the computation time without giving concessions from the accuracy. Boules et al., [12], obtain the solution for a specific boundary regime and initial conditions. Using a truncated Fourier series expansion yields an autonomous ODE set, the solution of which approximates the numerical solution, and the derived model rebuilds the situation implied by the chosen initial and boundary conditions. Except [12], the works on 2D Burgers equation emphasize the similar difficulties as the motivating factors and focus on the solutions and solvability issues. The current paper, on the other hand, derives a non-autonomous ODE model that has external inputs explicitly and that is valid for some set of boundary conditions with zero initial conditions.

When the 1D version is taken into consideration, it is seen that the 1D Burgers equation has previously been considered for modeling and control system design purposes, and it has been shown in [13] and the references therein that the task is achievable, yet there are very few results reporting the modeling issues for vector PDE sets and higher dimensional cases as emphasized above. This paper fills the gap between very simple models such as 1D heat flow or Burgers system and very complicated systems like those reported in [3, 14, 15, 16]. The presented work is a step towards the goal of modeling and control of more complicated PDE systems.

The current paper approaches the modeling problem from a control specialist's point of view, i.e. a suitable model reduction associated with a set of well-defined system inputs and a well-defined range of operating region. This process contains three major issues that need to be addressed appropriately. First issue is to collect the representative data and to exploit decomposition techniques for obtaining a set of ODEs. The next issue is to separate the effect of external stimuli from the other terms by utilizing the boundary conditions. The last issue is to validate the model. The process is continuous over a physical domain ($\Omega := [0,1]\times[0,1]$), the corners of which are the possible entries of external stimuli for both $u(x,y,t)$ and $v(x,y,t)$. Choosing an adequately dense grid, say Ω_d, makes it possible to obtain a finite element representation of the process $w(x,y,t)$ over Ω_d. When the content of the observed data, say $w(x,y,t)$, is decomposed into spatial and temporal constituents ($u(x,y,t) \approx \langle \Phi(x,y), \alpha(t) \rangle_{\Omega_d}$ and $v(x,y,t) \approx \langle \Psi(x,y), \alpha(t) \rangle_{\Omega_d}$), the essence of spatial behavior appears as a set of spatially varying gains ($\Phi(x,y) = \{\Phi_1(x,y), \Phi_2(x,y), \ldots, \Phi_{R_L}(x,y)\}$ and $\Psi(x,y) = \{\Psi_1(x,y), \Psi_2(x,y), \ldots, \Psi_{R_L}(x,y)\}$ with R_L being a positive integer), and the essence of temporal evolution, $\alpha(t)$, appears as the solution of a set of ODEs obtained after utilizing the orthogonality properties of the spatial basis functions, i.e. the eigenfunctions.

The dimension reduction in systems having high orders can be done by utilizing Proper Orthogonal Decomposition (POD) or Singular Value Decomposition (SVD) in cooperation with Galerkin projection [14, 15, 16] or balancing methods (for linear systems) as discussed in the survey of Gügercin, [17]. The decomposition based methods exploit the exemplar solutions obtained from the process and yield a set of temporal variables associated with a set of spatial basis functions. In order to obtain a useful approximation, the data, which is the raw information entering the modeling process, should contain coherent modes. The procedure, if it succeeds, yields a set of autonomous ODEs synthesizing the aforementioned temporal values.

The motivation of this paper is to draw a clear path between a given PDE system and the representative finite dimensional non-autonomous ODE model. With this in mind, the paper is organized as follows: The second section presents briefly the POD technique and its relevance to the modeling strategy. In the third section, obtaining the ODE model for the 2D Burgers equation is demonstrated. The justification of the model, results and the contributions are discussed in Section 4. The control system design and the results are presented in the 5th section. The concluding remarks constitute the last part of the paper.

2 Proper Orthogonal Decomposition

Consider the 2D Burgers equation given in (1), or more explicitly:

$$u_t = \mu u_{xx} + \mu u_{yy} - \epsilon u u_x - \epsilon v u_y \ , \quad v_t = \mu v_{xx} + \mu v_{yy} - \epsilon u v_x - \epsilon v v_y, \tag{2}$$

with ϵ and μ being known constants, and the subscripts $_x$, $_y$ and $_t$ refer to the partial differentiation with respect to x, y and time, respectively. The continuous time process takes place over the physical domain $\Omega := \{(x,y)|(x,y) \in [0,1] \times [0,1]\}$ and the solution is obtained on a grid denoted by Ω_d, which describes the coordinates of the pixels of every snapshot in the ensemble.

The goal is to find an orthonormal basis set letting us to write the solution as

$$\begin{pmatrix} u(x,y,t) \\ v(x,y,t) \end{pmatrix} \approx \begin{pmatrix} \hat{u}(x,y,t) \\ \hat{v}(x,y,t) \end{pmatrix} = \sum_{i=1}^{R_L} \alpha_i(t) \begin{pmatrix} \Phi_i(x,y) \\ \Psi_i(x,y) \end{pmatrix} \tag{3}$$

where $\alpha_i(t)$ is the temporal part, $\begin{pmatrix} \Phi_i(x,y) \\ \Psi_i(x,y) \end{pmatrix}$ is the spatial part, $\begin{pmatrix} \hat{u}(x,y,t) \\ \hat{v}(x,y,t) \end{pmatrix}$ is the finite element approximate of the infinite dimensional PDE and R_L is the number of independent basis functions that can be synthesized from the given ensemble, or equivalently the set of eigenfunctions that spans the space described by the ensemble. It will later be clear that if the elements of the basis set, $\begin{pmatrix} \Phi_i(x,y) \\ \Psi_i(x,y) \end{pmatrix}$, are orthonormal for $i = 1, 2, \ldots, R_L$, then the modeling task can exploit Galerkin projection technique. More explicitly, the inner product operator defined in over the basis functions should function as,

$$\langle \begin{pmatrix} \Phi_i \\ \Psi_i \end{pmatrix}, \begin{pmatrix} \Phi_j \\ \Psi_j \end{pmatrix} \rangle_\Omega := \iint_\Omega (\Phi_i \Phi_j + \Psi_i \Psi_j) \, d\Omega = \delta_{ij} \tag{4}$$

where $\delta_{ij} = 1$ when $i = j$ and zero otherwise, i.e. the Kronecker delta. With these definitions, the POD procedure can be summarized as follows:

Step 1. Define the concatenated process snapshot captured at time t_k as $P_k := \begin{pmatrix} U_k \\ V_k \end{pmatrix}$, where U_k and V_k are $R \times R$, P_k is $2R \times R$ and R determines the spatial resolution. Without loss of generality, k could be an integer that is used to index the snapshots. Start calculating the $N_s \times N_s$ dimensional correlation matrix L, the (ij)-th entry of which is $L_{ij} := \langle P_i, P_j \rangle_{\Omega_d}$, where $\langle ., . \rangle_{\Omega_d}$ is the inner product operator defined over the chosen spatial grid Ω_d. Notice that the basis vectors $\begin{pmatrix} \Phi_i(x,y) \\ \Psi_i(x,y) \end{pmatrix}$ are defined over Ω, whereas the bases that are obtained numerically (the sampled forms) $\begin{pmatrix} \phi_i \\ \psi_i \end{pmatrix}$ are defined over Ω_d and, ϕ_i and ψ_i are $R \times R$ matrices. Therefore, we need the equivalent form of the used inner product, which is given as

$$\langle \begin{pmatrix} \phi_i \\ \psi_i \end{pmatrix}, \begin{pmatrix} \phi_j \\ \psi_j \end{pmatrix} \rangle_{\Omega_d} := \frac{1}{N_s} (\phi_i \star \phi_j + \psi_i \star \psi_j) = \frac{1}{N_s} \sum_{p=1}^{R} \sum_{q=1}^{R} \phi_i(p,q)\phi_j(p,q) + \psi_i(p,q)\psi_j(p,q) = \delta_{ij}, \tag{5}$$

where $\star$ stands for the sum of all elements of a matrix that is obtained through elementwise multiplication of two matrices.

Step 2. Find the eigenvectors denoted by ξ_i and the associated eigenvalues (λ_i) of the symmetric matrix L. Sort them in a descending order in terms of the magnitudes of λ_i. Note that every ξ_i is an $N_s \times 1$ dimensional vector satisfying $\xi_i^T \xi_i = \frac{1}{\lambda_i}$, here, for simplicity of the exposition, we assume that the eigenvalues are distinct.

Step 3. Construct the basis set by utilizing the snapshots

$$\begin{pmatrix} \phi_i \\ \psi_i \end{pmatrix} = \sum_{k=1}^{N_s} \xi_{ik} P_k = \sum_{k=1}^{N_s} \begin{pmatrix} \xi_{ik} U_k \\ \xi_{ik} V_k \end{pmatrix}, \tag{6}$$

where ξ_{ik} is the k-th entry of the eigenvector ξ_i, and $i = 1, 2, \ldots, R_L$, where $R_L = \text{rank}(L)$. It can be shown that $\langle \begin{pmatrix} \phi_i \\ \psi_i \end{pmatrix}, \begin{pmatrix} \phi_j \\ \psi_j \end{pmatrix} \rangle_{\Omega_d} = \delta_{ij}$ with δ_{ij} being the Kronecker delta function. Notice that the basis functions are admixtures of the snapshots. [13, 16].

Step 4. Calculate the temporal coefficients. When $t = t_k$, taking the inner product of both sides of (3) with $\begin{pmatrix} \Phi_i \\ \Psi_i \end{pmatrix}$, the orthonormality property leads to

$$\alpha_i(t_k) = \langle \begin{pmatrix} \Phi_i(x,y) \\ \Psi_i(x,y) \end{pmatrix}, \begin{pmatrix} \hat{u}(x,y,t_k) \\ \hat{v}(x,y,t_k) \end{pmatrix} \rangle_\Omega = \langle \begin{pmatrix} \phi_i \\ \psi_i \end{pmatrix}, \begin{pmatrix} U_{t_k} \\ V_{t_k} \end{pmatrix} \rangle_{\Omega_d}, \tag{7}$$

Note that the temporal coefficients satisfy orthogonality properties over the discrete set $t_k \in \{t_1, t_2, \ldots, t_{N_s}\}$ (See (8)). For a more detailed discussion on the POD method, the reader is referred to [14, 15, 16] and the references therein,

$$\sum_{i=1}^{N_s} \langle \begin{pmatrix} U_i \\ V_i \end{pmatrix}, \begin{pmatrix} \phi_k \\ \psi_k \end{pmatrix} \rangle_{\Omega_d}^2 \approx \sum_{i=1}^{N_s} \alpha_i^2(t_i) = \lambda_k. \tag{8}$$

Fundamental Assumption: The majority of works dealing with POD and model reduction applications presume that the flow is dominated by coherent modes and the quantities $\begin{pmatrix} u(x,y,t) \\ v(x,y,t) \end{pmatrix}$ and $\begin{pmatrix} \hat{u}(x,y,t) \\ \hat{v}(x,y,t) \end{pmatrix}$ are indistinguishable, [14, 15, 16]. Because of the dominance of coherent modes, the typical spread of the eigenvalues of the correlation matrix L turns out to be logarithmic and the terms decay very rapidly in magnitude. This fact further enables to assume that a reduced order representation, say with M modes ($M \leq \min(R_L, N_s)$) can also be written as an equality

$$\begin{pmatrix} \hat{u}(x,y,t) \\ \hat{v}(x,y,t) \end{pmatrix} = \sum_{i=1}^{M} \alpha_i(t) \begin{pmatrix} \Phi_i(x,y) \\ \Psi_i(x,y) \end{pmatrix}, \tag{9}$$

and the reduced order model is derived under the assumption that (9) satisfies the governing PDE set. Unsurprisingly, such an assumption results in a model having uncertainties, however, one should keep in mind that the goal is to find a model, which matches the infinite dimensional system in some sense of approximation with typically $M \ll R_L \leq N_s$. To represent how good such an expansion is, a percent energy measure is defined as follows

$$E = 100 \frac{\sum_{i=1}^{M} \lambda_i}{\sum_{i=1}^{R_L} \lambda_i}, \tag{10}$$

where the tendency of $E \to 100\%$ means that the model captures the dynamical information contained in the snapshots well. Conversely, an insufficient model will be obtained if E is far below 100%. In the next section, we demonstrate how the boundary condition is transformed to an explicit control input in the ODEs.

3 Obtaining the ODE Model

The underlying assumption of POD based model reduction scheme is that the approximate solution (9) must satisfy (2). Substituting (9) into (2) and taking the inner product of both sides with $\begin{pmatrix} \Phi_k \\ \Psi_k \end{pmatrix}$ yields,

$$\begin{aligned} \dot{\alpha}_k &= \mu \sum_{i=1}^{M} \alpha_i \langle \begin{pmatrix} \Phi_{xx_i} + \Phi_{yy_i} \\ \Psi_{xx_i} + \Psi_{yy_i} \end{pmatrix}, \begin{pmatrix} \Phi_k \\ \Psi_k \end{pmatrix} \rangle_\Omega - \epsilon \sum_{i=1}^{M} \sum_{j=1}^{M} \alpha_i \alpha_j \langle \begin{pmatrix} \Phi_i \Phi_{xj} \\ \Phi_i \Psi_{xj} \end{pmatrix}, \begin{pmatrix} \Phi_k \\ \Psi_k \end{pmatrix} \rangle_\Omega \\ &\quad - \epsilon \sum_{i=1}^{M} \sum_{j=1}^{M} \alpha_i \alpha_j \langle \begin{pmatrix} \Psi_i \Phi_{yj} \\ \Psi_i \Psi_{yj} \end{pmatrix}, \begin{pmatrix} \Phi_k \\ \Psi_k \end{pmatrix} \rangle_\Omega. \end{aligned} \tag{11}$$

Notice that, the orthonormality property of the basis vectors leaves the $\dot{\alpha}_k$ term alone on the left hand side. Equivalently, by using the numerical quantities, the expression above can be rewritten as follows:

$$\begin{aligned} \dot{\alpha}_k &= \mu \sum_{i=1}^{M} \alpha_i \langle \begin{pmatrix} \phi_{xx_i} + \phi_{yy_i} \\ \psi_{xx_i} + \psi_{yy_i} \end{pmatrix}, \begin{pmatrix} \phi_k \\ \psi_k \end{pmatrix} \rangle_{\Omega_d} - \epsilon \sum_{i=1}^{M} \sum_{j=1}^{M} \alpha_i \alpha_j \langle \begin{pmatrix} \phi_i \circ \phi_{xj} \\ \phi_i \circ \psi_{xj} \end{pmatrix}, \begin{pmatrix} \phi_k \\ \psi_k \end{pmatrix} \rangle_{\Omega_d} \\ &\quad - \epsilon \sum_{i=1}^{M} \sum_{j=1}^{M} \alpha_i \alpha_j \langle \begin{pmatrix} \psi_i \circ \phi_{yj} \\ \psi_i \circ \psi_{yj} \end{pmatrix}, \begin{pmatrix} \phi_k \\ \psi_k \end{pmatrix} \rangle_{\Omega_d} \end{aligned} \tag{12}$$

where $\circ$ stands for the elementwise multiplication of two matrices.

Although it is straightforward to conclude with the ODEs given in (11) and (12), it is apparent that these equations do not have the boundary conditions (external inputs) explicitly. Chosen initial conditions and boundary excitation regime determine the solution, and the ODEs above re-synthesize the temporal variables, $\alpha_i(t)$, associated to that particular solution (See (9)). It is clear that such an ODE model is useless as it is specific to the chosen boundary conditions. Our goal is to obtain a model that has external inputs explicitly and that can be used for the boundary conditions other than the used ones. For this purpose, a method needs to be postulated for separating the boundary excitations appropriately. According to the definition of the inner product operator, it should be obvious that

$$\langle \begin{pmatrix} \phi_i \\ \psi_i \end{pmatrix}, \begin{pmatrix} \phi_j \\ \psi_j \end{pmatrix} \rangle_{\Omega_d} = \langle \begin{pmatrix} \phi_i \\ \psi_i \end{pmatrix}, \begin{pmatrix} \phi_j \\ \psi_j \end{pmatrix} \rangle_{\Omega_d \setminus \partial\Omega_d} + \langle \begin{pmatrix} \phi_i \\ \psi_i \end{pmatrix}, \begin{pmatrix} \phi_j \\ \psi_j \end{pmatrix} \rangle_{\partial\Omega_d} \tag{13}$$

where $\partial\Omega_d$ indicates the boundaries of the considered domain. Apparently, the last term in (13) can enjoy the boundary conditions that are specified freely. Denote (x_c, y_c) as one of the points at which the solution is independently specified (i.e. the boundary), and (p_{x_c}, q_{y_c}) as the row and column numbers of this location in matrices ϕ_i and ψ_i. Note that the prescribed solution in (9) must be satisfied also at (x_c, y_c), i.e. we have,

$$\hat{u}(x_c, y_c, t) := \gamma_{x_c y_c u}(t) = \sum_{i=1}^{M} \alpha_i(t)\phi_i(p_{x_c}, q_{y_c}) \qquad \text{and} \qquad \hat{v}(x_c, y_c, t) := \gamma_{x_c y_c v}(t) = \sum_{i=1}^{M} \alpha_i(t)\psi_i(p_{x_c}, q_{y_c}) \tag{14}$$

or equivalently

$$\alpha_k(t)\phi_k(p_{x_c}, q_{y_c}) = \gamma_{x_c y_c u}(t) - \sum_{i=1}^{M} (1 - \delta_{ik})\, \alpha_i(t)\phi_i(p_{x_c}, q_{y_c}), \tag{15}$$

$$\alpha_k(t)\psi_k(p_{x_c}, q_{y_c}) = \gamma_{x_c y_c v}(t) - \sum_{i=1}^{M} (1 - \delta_{ik})\, \alpha_i(t)\psi_i(p_{x_c}, q_{y_c}). \tag{16}$$

Since we consider the problem on a square domain, Ω_d, for both states, every corner can be a possible entry for the external excitations, i.e. we may have at most eight distinct inputs for this system. Once the Dirichlét type corner conditions are specified, the numerical solutions $u(x, y, t)$ and $v(x, y, t)$ on $x = 0$, $y = 0$, $x = 1$ and $y = 1$ segments of Ω_d are obtained by setting the relevant partial derivatives to zero. For example, we solve

$$u_t = \mu u_{yy} - \epsilon v u_y \quad \text{and} \quad v_t = \mu v_{yy} - \epsilon v v_y \tag{17}$$

along $x = 1$ segment. For the simplicity of the exposition, assume $x_c = 0$ and $y_c = 0$ ($(p_{x_c}, q_{y_c}) = (1, 1)$) is the chosen corner, and rewrite (12) as follows:

$$\begin{aligned} \dot{\alpha}_k \;=\; & \tfrac{\mu}{N_s} \textstyle\sum_{i=1}^{M} \alpha_i \left(\zeta_i \star \phi_k + \theta_i \star \psi_k\right) - \tfrac{\epsilon}{N_s} \sum_{i=1}^{M} \sum_{j=1}^{M} \alpha_i \alpha_j \left((\phi_i \circ \phi_{xj} + \psi_i \circ \phi_{yj}) \star \phi_k\right) \\ & - \tfrac{\epsilon}{N_s} \textstyle\sum_{i=1}^{M} \sum_{j=1}^{M} \alpha_i \alpha_j \left((\phi_i \circ \psi_{xj} + \psi_i \circ \psi_{yj}) \star \psi_k\right). \end{aligned} \tag{18}$$

where $\zeta_i := \phi_{xxi} + \phi_{yyi}$ and $\theta_i := \psi_{xxi} + \psi_{yyi}$. Define $\phi'_k = \{\phi'_k | \phi'_k(i,j) = \phi_k(i,j) \;\text{ when }\; i \neq p_{x_c}, j \neq q_{y_c}, \;\text{ and }\; \phi'_k(p_{x_c}, q_{y_c}) = 0\}$ and $\zeta'_k = \{\zeta'_k | \zeta'_k(i,j) = \zeta_k(i,j) \;\text{ when }\; i \neq p_{x_c}, j \neq q_{y_c}, \;\text{ and }\; \zeta'_k(p_{x_c}, q_{y_c}) = 0\}$ and so on. By this means, the matrices used in the derivation have zero values corresponding to the external excitation entries. Now we can explicitly write the first term in (18) as follows:

$$\sum_{i=1}^{M} \alpha_i \zeta_i \star \phi_k = \sum_{i=1}^{M} \alpha_i \left(\zeta'_i \star \phi'_k\right) + \alpha_k \zeta_k(1,1)\phi_k(1,1) + \sum_{i=1}^{M} (1 - \delta_{ik})\alpha_i \zeta_i(1,1)\phi_k(1,1). \tag{19}$$

Utilizing (15) for the term $\alpha_k \zeta_k(1,1)\phi_k(1,1)$, we get

$$\alpha_k \zeta_k(1,1)\phi_k(1,1) = \gamma_{00u}(t)\zeta_k(1,1) - \sum_{i=1}^{M} (1 - \delta_{ik})\alpha_i \zeta_k(1,1)\phi_i(1,1). \tag{20}$$

Inserting (20) into (19) yields the following

$$\sum_{i=1}^{M} \alpha_i \zeta_i \star \phi_k = \gamma_{00u}(t)\zeta_k(1,1) + \sum_{i=1}^{M} \alpha_i \left(\zeta_i \star \phi_k - \zeta_k(1,1)\phi_i(1,1)\right). \tag{21}$$

For the second term in the first summation of (18), this result implies the equality in (22), and the concatenated form is given in (23),

$$\sum_{i=1}^{M} \alpha_i(\theta_i \star \psi_k) = \gamma_{00v}(t)\theta_k(1,1) + \sum_{i=1}^{M} \alpha_i \left(\theta_i \star \psi_k - \theta_k(1,1)\psi_i(1,1)\right). \tag{22}$$

$$\begin{aligned}\textstyle\sum_{i=1}^{M} \alpha_i(\zeta_i \star \phi_k + \theta_i \star \psi_k) \;=\; & \gamma_{00u}(t)\zeta_k(1,1) + \gamma_{00v}(t)\theta_k(1,1) + \textstyle\sum_{i=1}^{M} \alpha_i(\zeta_i \star \phi_k) \\ & - \textstyle\sum_{i=1}^{M} \alpha_i(\zeta_k(1,1)\phi_i(1,1) + \theta_k(1,1)\psi_i(1,1)).\end{aligned} \tag{23}$$

The same reasoning can be applied to the terms seen in the second and third lines of (18). Due to the space limit, we skip repeating the same step. Such a separation technique lets us obtain the low dimensional model for the 2D Burgers equation given by

$$\dot{\mathcal{X}}(t) = \mathcal{A}\mathcal{X}(t) - \mathcal{B}(\mathcal{X}(t)) + \mathcal{C}\Gamma(t) - \mathcal{D}(\mathcal{X}(t), \Gamma(t)), \tag{24}$$

where $\mathcal{X}(t) = \begin{pmatrix} \alpha_1(t) & \alpha_2(t) & \dots & \alpha_M(t) \end{pmatrix}^{\mathsf{T}}$, $\Gamma(t) = \begin{pmatrix} \gamma_{00u}(t) & \gamma_{00v}(t) \end{pmatrix}^{\mathsf{T}}$, $\mathcal{A}$ is $M \times M$, $\mathcal{B}$ is $M \times 1$, $\mathcal{C}$ is $M \times 2$ and $\mathcal{D}$ is $M \times 1$. From (23), we can write the (ki)-th entry of matrix $\mathcal{A}$ and k-th row of matrix $\mathcal{C}$ as given below:

$$(\mathcal{A})_{ki} = \frac{\mu}{N_s}(\zeta_i \star \phi_k + \theta_i \star \psi_k) - \frac{\mu}{N_s}(\zeta_k(1,1)\phi_i(1,1) + \theta_k(1,1)\psi_i(1,1)), \tag{25}$$

$$(\mathcal{C})_k = \frac{\mu}{N_s}(\zeta_k(1,1) \;\; \theta_k(1,1)). \tag{26}$$

where $k, i = 1, 2, \dots, M$. Similarly,

$$\mathcal{B}(\mathcal{X}) = \begin{pmatrix} \mathcal{X}^{\mathsf{T}}B_1\mathcal{X} & \mathcal{X}^{\mathsf{T}}B_2\mathcal{X} & \dots & \mathcal{X}^{\mathsf{T}}B_M\mathcal{X} \end{pmatrix}^{\mathsf{T}} \tag{27}$$

where the j-th of matrix B_k is

$$(B_k)_{ij} = \frac{\epsilon}{N_s}(\phi'_i \circ \phi'_{xj}) \star \phi'_k + \frac{\epsilon}{N_s}(\psi'_i \circ \phi'_{yj}) \star \phi'_k + \frac{\epsilon}{N_s}(\phi'_i \circ \psi'_{xj}) \star \psi'_k + \frac{\epsilon}{N_s}(\psi'_i \circ \psi'_{yj}) \star \psi'_k, \tag{28}$$

and we can show that

$$\mathcal{D} = D_u\mathcal{X}\gamma_{00u} + D_v\mathcal{X}\gamma_{00v} \tag{29}$$

where D_u and D_v are $M \times M$ matrices and the (kj)-th entry is computed as

$$(D_u)_{kj} = \frac{\epsilon}{N_s}(\phi_k(1,1)\phi_{xj}(1,1) + \psi_k(1,1)\psi_{xj}(1,1)), \tag{30}$$

$$(D_v)_{kj} = \frac{\epsilon}{N_s}(\phi_k(1,1)\phi_{yj}(1,1) + \psi_k(1,1)\psi_{yj}(1,1)). \tag{31}$$

with $k, j = 1, 2, \dots, M$. According to the derivation discussed in this section, once the initial and boundary conditions are specified, one can get a dynamic model that captures the essential features contained by the solution. Although we have derived the model by assuming the external excitation enters at a single point for u and v dynamics, it is straightforward to apply the scheme for obtaining a model having up to eight inputs. In the next section, justification of the model is presented through some exemplar cases.

4 Justification of the Model

In order to obtain the model, the 2D Burgers equation in (1) is solved for the boundary conditions given as

$$\gamma_{00u}(t) = \sin(1000\pi t(T-t)) \quad \text{and} \quad \gamma_{00v}(t) = \cos(1000\pi t(\frac{T}{2} - t)). \tag{32}$$

The time plots and the Fast Fourier Transforms (FFT) of the signals above are depicted in Figure 1. The reason that drives us to choose such signals is the spectral richness. If the spectral content of the excitations are rich enough, the resulting model is more likely to operate properly over the covered frequency range, [13]. The other important parameters of the simulation are tabulated in Table 1. The

Table 1: Simulation Settings

R	M	ΔT	T	N_s	ϵ	μ
25	8	0.1 msec.	0.2 sec.	201	1	5

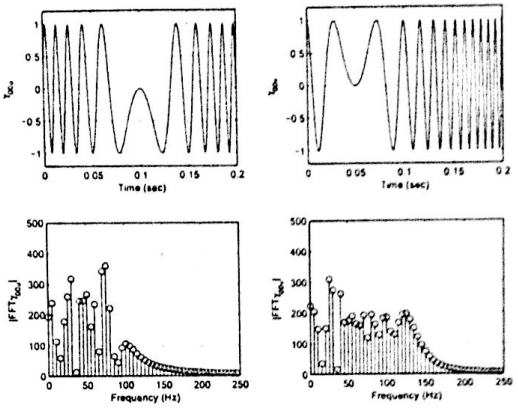

Figure 1: Boundary signals used for model derivation

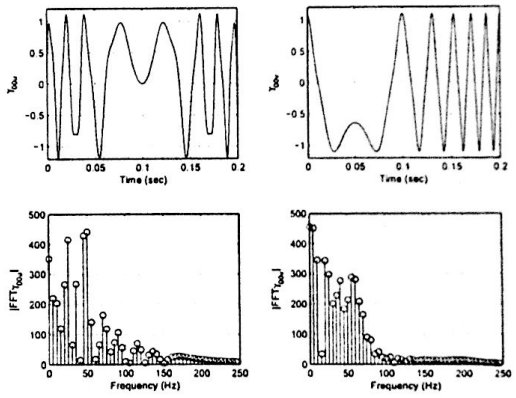

Figure 2: First set of boundary signals that are used for model validation

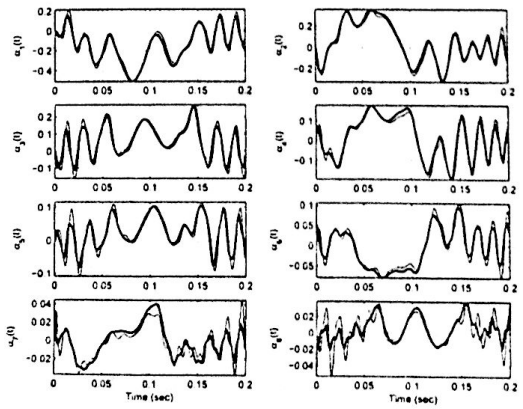

Figure 3: The desired values (thick curves) of $\alpha_i(t)$ and the obtained values (thin curves): first test conditions

numerical solution is obtained through Crank-Nicholson method with zero initial conditions, [18], and after the application of the modeling procedure discussed in the previous section, a model is obtained in the form of (24). It has been observed that the eigenvalues (λ_i) decay very rapidly, and the captured energy content described by (10) is 99.9021%, which is found acceptable. The justification has been done with the same settings as shown in Table 1, and the first set of boundary excitations that are used in the model validation phase are

$$\begin{aligned} \gamma_{00u}(t) &= \sin(700\pi t(T-t)) + 0.2\sin(1700\pi t(T-t)), \qquad \text{and} \\ \gamma_{00v}(t) &= \cos(500\pi t(\tfrac{T}{2}-t)) + 0.1\cos(1500\pi t(\tfrac{T}{2}-t)). \end{aligned} \tag{33}$$

Figure 2 illustrates these signals and the low frequency appearance of their FFT magnitude plots. The PDE is solved for this new case and the $\alpha_i(t)$ values are obtained by using (7), which yield the desired values. On the other hand, the model had already been developed, and it is simulated for the test boundary conditions in (33) with zero initials. The outcome is expected to approximate the desired ones if the algorithm succeeds. The results are shown in Figure 3, where the first remark of us is the number of ODEs that let us obtain this result. With $M = 8$ modes (ODEs), the task can be achieved to the extent seen in the figure. For the first five modes, the match is quite good yet as the mode number increases the dissimilarity between the desired and generated values become more distinguishable. Since the dominance of the corresponding modes decrease logarithmically, as seen from the figure as well, so do their effect on the overall result. Therefore the similarity of the first few modes is more substantial than the similarity of modes having high index numbers. A rough look at the eight subplots of Figure 3 altogether gives the idea of a successful approximation from a higher dimensionality to low orders, which is the goal of this paper.

We have repeated our tests for many other test signals but some of them have driven us to conclude with the relevance of model performance and spectral content of the external excitations. The descriptive nature of the signals used in the model derivation is inherited by the developed dynamical model, and the signals that do not resemble to the model derivation conditions make the system fail depending on the level of dissimilarity between the model derivation and validation signals. The spectral dependence is an important conclusion if the model is to be used in a feedback system synthesis. This claim has been justified by choosing signals that are spectrally similar to and dissimilar from the test conditions.

According to the results of this paper, it is fair to claim that the dynamic model in (24) functions properly up to 100 Hz. Considering the results obtained in [12], it is seen that the presented work achieves the modeling goal with a few ODEs and associated spatial eigenfunctions.

A natural issue that needs to be highlighted is the ways of improving obtained results. Expectedly, increasing the grid fineness, decreasing Δt, increasing the number of snapshots entering the POD procedure (N_s), increasing the number of modes (M) are the alternatives that result in better model performance yet the price paid for this improvement is the increased computational requirements.

5 Control Studies

In the control system design section of this study, we consider the low dimensional model in (24), and linearize it around $\alpha = 0$. This yields the following MIMO linear system

$$\dot{\mathcal{X}}(t) = \mathcal{A}\mathcal{X}(t) + \mathcal{C}\Gamma(t), \qquad \hat{u} = \mathcal{F}_u\mathcal{X}, \qquad \hat{v} = \mathcal{F}_v\mathcal{X}, \tag{34}$$

where $\mathcal{F}_u = \begin{pmatrix} \Phi_1(x_m, y_m) & \dots & \Phi_M(x_m, y_m) \end{pmatrix}$ and $\mathcal{F}_v = \begin{pmatrix} \Psi_1(x_m, y_m) & \dots & \Psi_M(x_m, y_m) \end{pmatrix}$ with x_m and y_m being the spatial coordinates of chosen measurement point. The system is under an ordinary feedback loop with zero reference signal. We design feedback controller to attenuate the load disturbance entering the loop at the control input of the system. For this purpose, we analyzed the gain margin of the two transfer functions, namely the one from γ_{00u} to $\hat{u}(x_m, y_m, t)$ (System U) and the one from γ_{00v} to $\hat{v}(x_m, y_m, t)$ (System V). Such an approach discards the cross couplings and postulates the controller in terms of the linearized and simplified models of the PDE process.

Choosing $x_m = y_m = 0.5$ and considering the root locus for both of the linearized systems, System V has a smaller gain margin compared to that of System U. From the root locus plot, the value of the proportional gain bringing the closed loop system at the verge of instability is determined approximately about 30 and this result is in very good compliance with the simulations carried out with $K_p = 30$. This result implies that the linearized model represents the actual nonlinear system with sufficient degrees

of accuracy. The simulations have demonstrated that the sole P (proportional) control action is not sufficient to accomplish the disturbance rejection task. For this reason, we consider the PI (proportional + integral) type of a control action. The extensive simulation results for PI control suggest that it might be possible to obtain an optimal configuration for $K_p - K_i$ pair (PI gains). This can be achieved by a search for the optimal configuration using fast response and small error at a relatively short time as the criterion, and such a trial and error based grid search terminates at $K_p = 5$ and $K_i = 205$. The simulation results demonstrating the performance of the closed loop control system are shown in Figure 4.

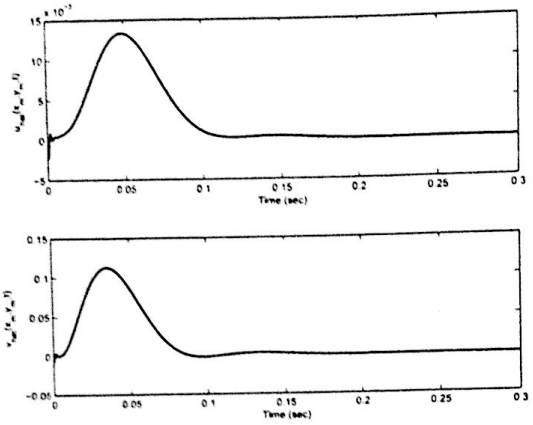

Figure 4: The compensation of the step disturbance occuring at the beginning of the simulation

A closer look at the figure stipulates that the disturbance corrupting both γ_{00u} and γ_{00v} has a visible effect at the measurement location. According to the results seen in the figure, the controller is able to compensate the deficiencies caused by the load disturbance within 0.15 seconds, which is the best result encountered during the parameter search process.

6 Conclusions

This paper focuses on the low dimensional modeling and control of 2D Burgers equation. The driving fact for focusing on this system is its similarity to Navier-Stokes equations, and its nonlinear, coupled and vector valued PDE nature. Once the POD algorithm is implemented, it is seen that the resulting ODE model is an autonomous one, that is the control input is implicit in the dynamical equations. One major contribution of this paper is on the separation of boundary terms to obtain a non-autonomous ODE model which demonstrates the effect of the the external control input explicitly. The second contribution of the paper is its emphasis on the locality of the developed low order models. It is seen that the conditions used in the model derivation are critically important and the POD procedure has a natural propensity to build models that are valid on particular conditions. With these results, the present work advances the subject area to the establishment of a clear connection between state-space methods of control theory and complex infinite dimensional systems of PDEs. The fact that this connection is built through the numerical observations from the infinite dimensional process is worthwhile to stress the applicability of the bottom-up modeling effort for other systems of PDEs. Finally, the linearization based feedback control of the system is considered. The simulation results have shown that PI controller with the determined K_p and K_i is able to suppress the undesired effect of the disturbance in a very short while.

Acknowledgments: The author would like to thank Prof. M. Samimy, Drs. J.H. Myatt, J. DeBonis, R.C. Camphouse and P. Yan, for fruitful discussions.

References

[1] J. Donea and A. Huerta. *Finite Element Methods for Flow Problems*, John Wiley & Sons, West Sussex, pp.252-253, 2003.

[2] J.M. McDonough and M.T. Huang. A Poor Man's Navier-Stokes Equation: Derivation and Numerical Experiments-The 2D Case. *Int. J. for Numerical Methods in Fluids*, **44**, pp.545-578, 2004.

[3] M. Samimy, M. Debiasi, E. Caraballo, J. Malone, J. Little, H. Özbay, M.Ö. Efe, P. Yan, X. Yuan, J. Debonis, J.H. Myatt, and R.C. Camphouse. Exploring strategies for closed-loop cavity flow control. *42nd AIAA Aerospace Sciences Meeting and Exhibit*, January 5-8, Reno, Nevada, U.S.A., AIAA 2004-0576, 2004.

[4] Sirendaoreji. Exact solutions of the two-dimensional Burgers equation. *Journal of Physics A: Mathematical and General*, **32**, pp.6897-6900, 1999.

[5] L. Hietarinta. Comments on 'Exact solutions of the two-dimensional Burgers equation. *Journal of Physics A: Mathematical and General*, **33**, pp.5157-5158, 2000.

[6] Z. Zhu. Exact solutions for a two-dimensional KdV-Burgers-type equation. *Chinese Journal of Physics*, **34**, 4, pp.1101-1105, 1996.

[7] R. Blender. Iterative solution of nonlinear partial-differential equations. *Journal of Physics A: Mathematical and General*, **24**, 10, pp.L509-L512, 1991.

[8] F. Güngör. Symmetries and invariant solutions of the two-dimensional variable coefficient Burgers equation. *Journal of Physics A: Mathematical and General*, **34**, pp.4313-4321, 2001.

[9] K. Nishinari, J. Matsukidaira, and D. Takahashi. Two-dimensional Burgers cellular automaton. *Journal of the Physical Society of Japan*, **70**, 8, pp.2267-2272, 2001.

[10] I. Hataue. Mathematical and numerical analyses of dynamical structure of numerical solutions of two-dimensional fluid equations. *Journal of the Physical Society of Japan*, **67**, 6, pp.1895-1911, 1998.

[11] B.L. Wescott, Rizwan-uddin. An efficient formulation of the modified nodal integral method and application to the two-dimensional Burgers equation. *Nuclear Science and Engineering*, **139**, 3, pp.293-305, 2001.

[12] A.N. Boules and I.J. Eick. A spectral approximation of the two-dimensional Burgers equation. *Indian Journal of Pure & Applied Mathematics*, **34**, 2, pp.299-309, 2003.

[13] M.Ö. Efe and H. Özbay. Low dimensional modeling and Dirichlét boundary controller design for Burgers equation. *International Journal of Control*, **77**, 10, pp.895-906, 2004.

[14] S.S. Ravindran. A reduced order approach for optimal control of fluids using proper orthogonal decomposition. *Int. Journal for Numerical Methods in Fluids*, **34**, pp.425-488, 2000.

[15] S.N. Singh, J.H. Myatt, G.A. Addington, S. Banda, and J.K. Hall. Optimal feedback control of vortex shedding using proper orthogonal decomposition models. *Trans. of the ASME: Journal of Fluids Eng.*, **123**, pp.612-618, 2001.

[16] H.V. Ly, and H.T. Tran. Modeling and control of physical processes using proper orthogonal decomposition. *Mathematical and Computer Modelling of Dynamical Systems*, **33**, pp.223-236, 2001.

[17] S. Gügercin and A.C. Antoulas. A survey of model reduction by balanced truncation and some new results. *International Journal of Control*, v.77, no.8, pp.748766, 2004.

[18] S.J. Farlow, *Partial Differential Equations for Scientists and Engineers*, Dover Publications Inc., New York, pp.317-322, 1993.

[19] L. Baramov, O.R. Tutty, and E. Rogers. Robust control of linearized Poiseuille flow. *AIAA Journal of Guidance, Dynamics, and Control*, **25**, pp.145-151, 2002.

[20] O.M. Aamo, and M. Krstić. *Flow Control by Feedback*, Springer-Verlag London Limited, 2003.